

1 THREE DIMENSIONAL MEASUREMENTS OF ASPHALTENE DEPOSITION
2 IN A TRANSPARENT MICRO-CHANNEL

3 *Y. Zhuang*¹, *A. Goharzadeh*^{1*}, *Y. J. Lin*², *Yit F. Yap*¹, *J. C. Chai*^{1&}, *N. Mathew*³, *F. Vargas*²,
4 *Sibani L. Biswal*²

5 ¹Department of Mechanical Engineering, The Petroleum Institute, Abu Dhabi, United Arab Emirates,

6 ²Department of Chemical and Biomolecular Engineering, Rice University, TX, USA,

7 [&]Currently at School of Computing & Engineering, University of Huddersfield, Huddersfield, UK,

8 ³Department of Chemical Engineering, The Petroleum Institute, Abu Dhabi, United Arab Emirates.

9 This study describes a novel experimental approach to directly measure the thicknesses of
10 asphaltene deposits in micro-channels. The thickness of the asphaltene deposit is estimated using
11 a visualization technique based on 3D digital microscopy. The working fluid is a mixture of n-
12 heptane and dead oil. Induced by the addition of n-heptane, the asphaltenes present in crude oil
13 phase separate at ambient temperature to form aggregates of asphaltene-rich phase. Part of the
14 asphaltene aggregates deposit on the walls of the transparent micro-channel. A two-dimensional
15 profile of the deposit across the channel at selected axial sections is measured. The influences of
16 injection mixture volume on the growth of the thickness of deposited asphaltenes is investigated
17 using two experimental conditions, (i) varying elapsed time at constant flow rate and (ii)
18 increasing the flow rate at a constant elapsed time. In both cases the deposit thickness of
19 asphaltene (δ) increases with the total injection volume (V). The experimental results obtained in

1 this work provide new insights into the deposition process at the micro-scale level, which can be
2 used to facilitate the development of more accurate numerical model for this application.

3 **1. INTRODUCTION**

4 During the process of oil production, transportation and refinery, asphaltene aggregates are
5 formed at specific temperature and pressure conditions and deposit in the wellbore and the near-
6 wellbore region. This deposition can cause formation damage in reservoirs, blockage in
7 wellbores or even problem in separators, pumps, pipelines, heat exchangers and other equipment
8 (Akbarzadeh *et al.*, 2012). Therefore, understanding the mechanisms of asphaltene disposition
9 has direct impact on oil production and attracts considerable attention in petroleum engineering
10 (Papadimitriou *et al.*, 2007; Buckley, 2012), with the main objective of preventing the asphaltene
11 deposition. Combining effect of both thermodynamic and hydrodynamic parameters, coupled
12 with chemical reactions, forces the deposition process to be extremely difficult to model, predict
13 and prevent. To investigate the influence of hydrodynamic effects on asphaltene deposition, such
14 as interaction between asphaltene particles and solid walls, the rate of asphaltene deposition, or
15 shear stress of the deposits, micro-scale experiments are widely used and represent novel and
16 suitable systems (Jensen., 2001; Schneider *et al.*, 2013; Hu *et al.*, 2014). The utilizations of
17 micro-channels offer the advances in studying interfacial properties and intrinsic asphaltene
18 behaviors in straight micro-channels (Seifried *et al.*, 2013) and micro-porous media (Hu *et al.*,
19 2014).

20 In previous experimental studies, micro-scale devices have been used to quantify asphaltene
21 deposits and measure the deposition rate in stainless steel capillary tubes (Broseta *et al.*, 2000;
22 Wang *et al.*, 2004; Nabzar *et al.*, 2008 and Hoepfner *et al.* 2013), transparent glass capillary

1 tubes or micro-channels (Boek *et al.*, 2008; Boek *et al.*, 2009; Lawal *et al.*, 2012 and Buckley.,
 2 2012).

3 Both homogeneous and non-homogeneous deposits have been reported depending on
 4 experimental conditions. Table 1 shows a summary of experimental tests with corresponding
 5 experimental conditions.

6

7 **Table 1.** A summary of experimental tests with corresponding experimental conditions

Ref	Characteristics Length (µm)	Flow Rate (ml/min)	Velocity (m/s)	Reynolds Number
Broseta <i>et al.</i> (2000)	250	0.1 - 10	0.034 - 3.4	Crude Oil B: 0.998 - 99.8 Crude Oil F: 0.144-14.4
Wang <i>et al.</i> (2004)	508	0 - 3.33	0.274	-
Nabzar and Aguilera (2008)	116 - 520	0.25 - 4	0.039 - 1.577	Weyburn: 4.3 – 779 Arabian Light: 1.5 – 277 Hassi Messaoud: 3.9 - 708
Boek <i>et al.</i> (2008, 2009)	91	0.002 -0.01	0.0051 - 0.0256	<< 1
Lawal <i>et al.</i> (2012)	320	0.005 – 0.06	0.001 - 0.012	< 0.5
Seifried <i>et al.</i> (2013)	91	0.005	0.0012 - 0.0064	0.8
Buckley (2012)	36	0	0	0
Hoepfner <i>et al.</i> (2013)	254 or 762	0.6	0.022 - 0.197	A:0.18- 4.96 WY: 0.62-16.7

8

9 Broseta *et al.* (2000) reported asphaltene deposition using continuous flow in a capillary
 10 tube. Their experiments were conducted in a temperature- and pressure- controlled system in
 11 which pressure drops were measured and the deposit depths were calculated from the change in
 12 pressure drop as a result of asphaltene deposition. They observed that the rate of deposition
 13 increased with the distance from deposition onset. Nabzar and Aguilera (2008) used similar

1 capillary tubes and proposed general scaling laws. They observed that the deposit thickness was
2 increasing rapidly with the reduction of the shear rate. Lawal *et al.* (2012) visualized the
3 asphaltene deposition in transparent cylindrical glass capillary tubes and correlated the
4 deposition patterns with deposit thicknesses deduced from pressure drop measurements.

5 In above experimental studies, empirical models were developed to predict the thickness of
6 the asphaltene deposits based on indirect measurement techniques where the assumption of
7 uniform deposit thickness was the precondition. However recent experiments based on flow
8 visualization showed that the homogeneous deposition process hypothesis may not be valid. To
9 visualize asphaltene deposition processes, experiments using glass setups were carried out by
10 Boek *et al.* (2008, 2009) and Seifried *et al.* (2013). The asphaltene deposition was directly
11 visualized in a transparent rectangular micro-channel, as a function of the distance from the
12 capillary entrance. They concluded that the distribution of deposits was not uniform in space,
13 which decreased from the capillary entrance and also changed with time for a fixed flow rate.
14 Hoepfner *et al.* (2013) conducted a series of experiments with similar mixing conditions that
15 Buckley (2012) has used. They have visualized the highly non-uniform axial deposit profile
16 using scanning electron microscope (SEM), and found that the pressure drop increased with
17 increasing the elapsed time during the flow tests.

18 Wang *et al.* (2004) investigated deposition rate process. They observed that deposition rate
19 was independent of tube length and flow rate and relied on mixture super-saturation of oil and n-
20 alkanes. Jamialahmadi *et al.* (2009) have used non-isothermal conditions to estimate the mass of
21 asphaltene deposition by measuring heat transfer coefficient and the thermal resistance of the
22 asphaltene deposit. Their experimental results showed that the rate of deposition was
23 proportional to surface temperature and asphaltene concentration. However, they also observed

1 deposition rate increased when oil velocity was decreased. Seifried *et al.* (2013) suggested that
2 the asphaltene deposition rate was sensitive to the magnitude of the average mixture velocity at
3 the earlier experimental time. This early asphaltene behavior relied on the flux of particles
4 through the experimental setup. They also found that the influence of flow rate on deposition
5 thickness was almost negligible.

6 In experimental studies reported in Table 1, indirect measurement techniques have been
7 used to investigate the driving forces in the asphaltene deposition process and estimate the
8 amount of asphaltene deposits in micro-devices. The proposed visualization techniques were
9 mainly applied on studying asphaltene behaviors. However, the whole deposit profiles cannot be
10 measured since the used channels and capillary tubes were closed.

11 The objective of this study is to present an innovative method, which is still missing in the
12 literature, to directly measure the asphaltene deposit profiles by using a transparent micro-
13 channel coupled with a 3D microscope. The method describing 3D measurement techniques is
14 presented and applied to analyze the influence of total injection volume on asphaltene deposition.
15 Results for the effect of total injection volume on asphaltene deposit thickness are presented
16 using two different experimental conditions. This novel approach has facilitated the development
17 of accurate simulation for the growth of asphaltene deposits.

18 In what follows, the experimental setup is described first in section 2. The details of
19 measurement technique are presented in section 3. Finally, in section 4, experimental results,
20 validation and discussions on asphaltene deposition are presented.

21
22
23

2. EXPERIMENTAL METHODS

2.1 Experimental setup

The experimental setup consists of a vertical transparent microchannel (Figure 1), a dual-drive syringe pump having two glass syringes, a collection tank and a microscope for flow visualization. The microchannel was fabricated from Plexiglas and had the dimension of $250 \mu\text{m} \times 50 \text{ mm} \times 2 \text{ mm}$ (depth \times length \times width). In this study, the flow direction is from bottom to top. The syringe pump (Cole-Parmer with 106.6 mL/min maximum flow rate) is used to mix two fluids (crude oil and n-heptane) together to generate a mixing working fluid flowing at a designed flow rate. Glass syringes (SAMCO, 10 ml) and microchannel are connected through transparent plastic tubes and a T-junction. Both fluids were injected to the test section using the T-junction. The ratio of working fluids including crude oil and n-heptane is controlled by flow rates via the syringe pump. All experiments were conducted using a fixed injection ratio of crude oil : n-heptane (3:7). The range of flow rates used was between 0.003 to 0.008 ml/min while the experimental elapsed times from 4 to 14 hours were examined. The temperature of the working fluids is at a constant temperature of 21°C .

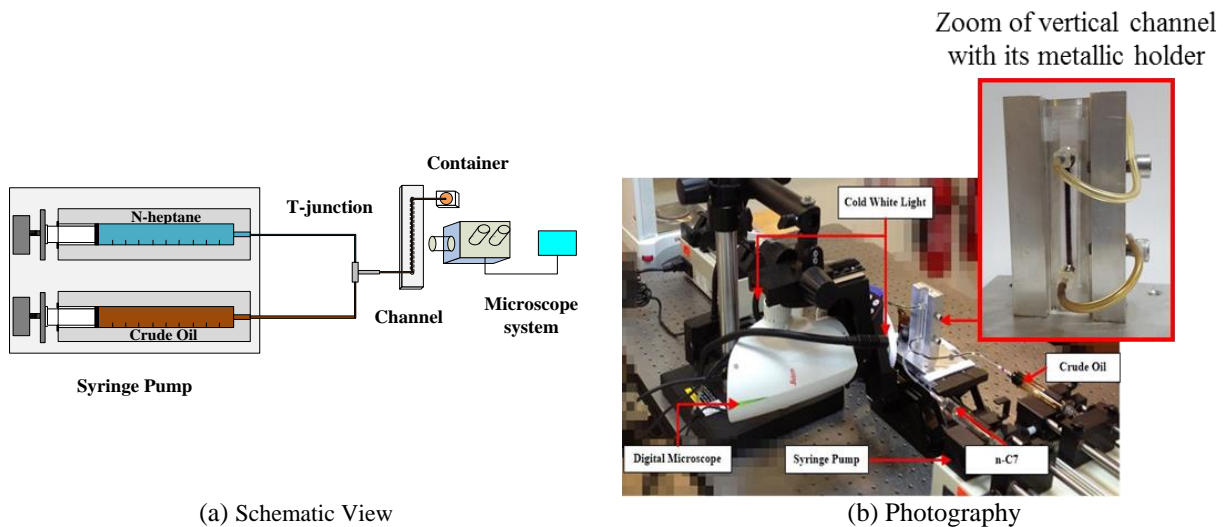


Fig. 1. Experimental setup representing the microchannel in vertical flow condition

1 **2.2 Crude oil preparation**

2 The oil samples used for these studies were found to be highly unstable (i.e., asphaltene
3 aggregates already formed in the crude oil) at the laboratory conditions. These asphaltene
4 aggregates are removed by centrifuging the crude oil for 15 minutes at an angular speed of 4000
5 rpm. The absence of major suspended particles was further confirmed by examining the
6 supernatant oil obtained after centrifugation using a Hirox KH7700 digital microscope. The oil
7 sample was then titrated under ambient conditions with an asphaltene precipitant such as n-
8 Heptane. In order to obtain the best ratio of oil to asphaltene precipitant, the oil sample was
9 titrated with n-Heptane in the ratios of 0:100 to 100:0 over an aging period of 5 minutes. Prior to
10 the deposition experiments, the fluid mixture ratio of 3:7, observed under normal microscope,
11 showed sufficient presence of asphaltene particles in the fluid mixture. A subsequent experiment
12 was confirmed that this ratio could create a quantifiable amount of deposits in the micro-channel
13 without blocking the experimental system for at least 14 hours (Zhuang *et al.* 2015 and Zhuang
14 2015). Properties of the crude oil, obtained from SARA analysis were reported in Table 2. The
15 determination of various components in the crude oil such as Saturates, Aromatics and Resins
16 were characterized by using ASTM D-2007m method and the Asphaltene component was
17 characterized by IP 143 method. The n-heptane precipitant has a density and kinematic viscosity
18 of 0.684 g/cm³ and 0.647 cSt, respectively. Both density and kinematic viscosity of the crude oil
19 were measured by ASTM D-4052 and ASTM D-445, respectively.

20 **Table 2.** Properties of Crude Oil

° API	Density at 20°C (g/cm ³)	Kinematic Viscosity (cSt)	Saturates (Wt. %)	Aromatics (Wt. %)	Resins (Wt. %)	Asphaltenes (Wt. %)
36.5	0.8412	6.505	49.9	14.2	5.6	0.4

21

22

1 **3. Measurement Technique using 3D Microscopy**

2 After a continuous deposition experiment, the syringe pump was stopped and all connectors
3 were removed from the microchannel. The microchannel was drained and then dried for 24 hours
4 under laboratory conditions. Once the channel was drained of liquid mixture, the top cover of the
5 channel was removed to facilitate measurements of asphaltene deposit in the channel. The
6 opened microchannel was therefore utilized for deposition thickness measurements. The 3D
7 scanning of asphaltene deposition was achieved by Hirox 3D digital microscope KH-7700 using
8 OL - 350 II lens with a maximum magnification lens of $\times 3500$ (Table 3).

9

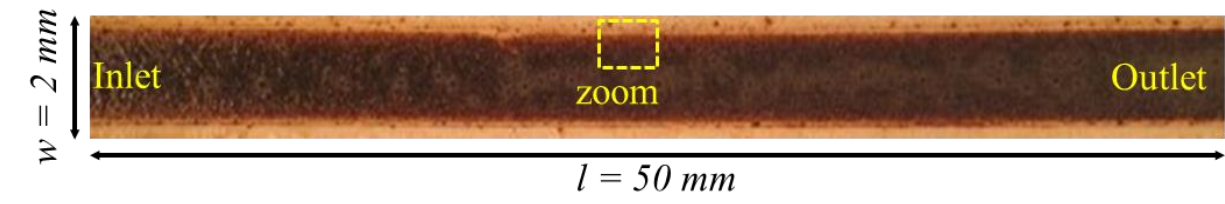
Table 3. Properties of the 3D digital microscope

Production Name	Hirox KH-7700
Use Lens Name	MX(G)-5040SZ: OL - 350 II
Magnification	350 - 3500 \times
Depth of Field (Optical)	762 μm to 90 μm

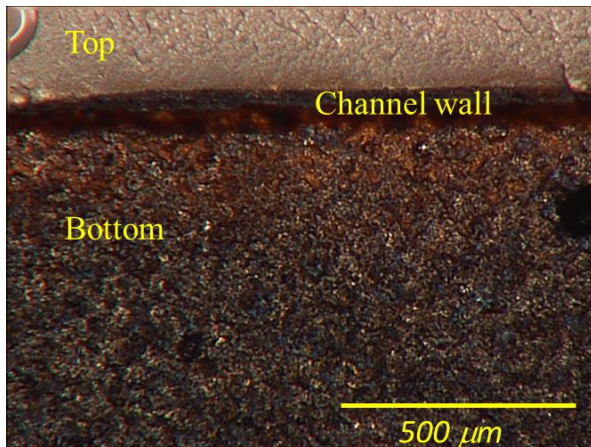
10

11 The microchannel is placed horizontally under the 3D microscope (Figure 2-a). A small
12 area of the microchannel (1240 by 930 μm^2) is selected and viewed under the 3D microscope.
13 The 3D microscope records images at a fixed position in the middle of the channel (at 25 mm
14 from the entrance). Using the 3D microscope software (Hirox-Real-Time 2D and 3D), the
15 bottom and top surfaces of the microchannel are defined by the user before performing a 3D scan
16 of the sample. The microscope starts from the very bottom surface of the sample and moves
17 upward at a constant interval distance until it reaches the very top surface of the sample. Interval
18 distance is determined relative to the distance between the bottom surface and the top surface.
19 Every image taken by the microscope has different zones with fully in and out of focus. The
20 height of each picture is recorded to construct the 3D structure of the deposition. A maximum of

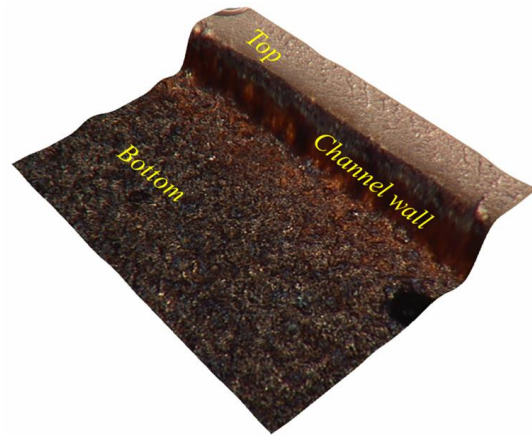
1 128 images can be taken by the microscope between the bottom and top surfaces. The smallest
 2 interval height increment between two images is $0.25 \mu\text{m}$. A reconstructed image of micro-
 3 channel in both two and three dimensions are obtained and presented in figure 2-b and 2-c,
 4 respectively. In order to visualize the three dimensional effect, figure 2-c is presented using an
 5 isometric 3D view of asphaltene layer deposited on the bottom wall of the micro-channel.



(a) Digital image of the entire channel



(b) Two dimensional view of the reconstructed image (the magnification is $\times 350$)



(c) Three dimensional Isometric view of the reconstructed image (the magnification is $\times 350$)

Fig. 2. Different view of the microchannel with asphaltene deposited on the wall.

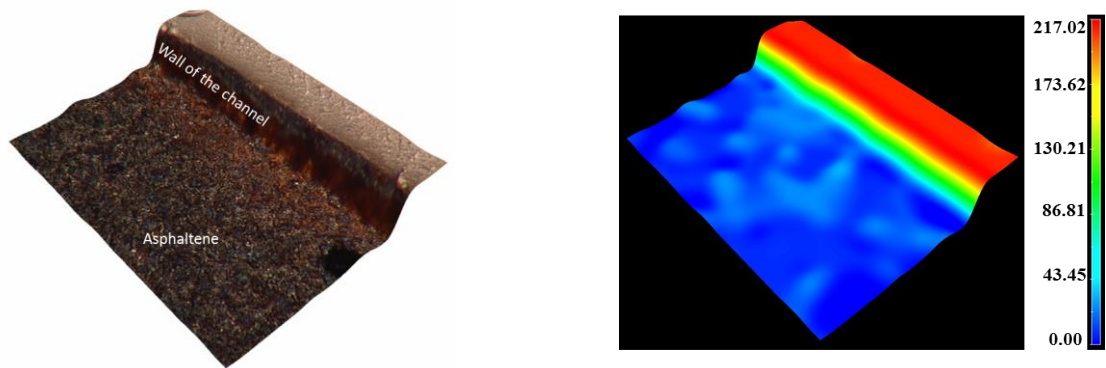
6

7 **4. Results and Discussions**

8 **4.1 2D profile of asphaltene deposit**

9 Figure 3-a represents a reconstructed image of 128 single images taken between the bottom
 10 and top surfaces; each image focused at different vertical positions of the channel. Due to the
 11 high magnification of the lens, only a very small region of the micro-channel is visible. The
 12 black area represents the deposited layer of asphaltene particles. As it can be observed in the

1 figure, the entire vertical wall of the mini-channel is also covered by a thin layer of asphaltene.
 2 In Figure 3-b, the depth of each layer of the asphaltene deposited on the bottom wall is measured
 3 and presented using a palette of colors. The legend is given with dimensions in micrometer. Blue
 4 and red represent the lowest and the highest vertical positions in the reconstructed image which
 5 correspond to the bottom and top surfaces of the channel respectively. Quantitative values of
 6 asphaltene deposition can be extracted from Figure 3 by plotting a 2D profile of the asphaltene
 7 deposited on the wall. The average value of the deposited asphaltene layer can be obtained by
 8 comparing the measurement with thickness of the empty channel. Figure 4 represents two
 9 pictures of the 3D image of an empty microchannel and a microchannel with deposits. Both
 10 pictures were captured in the same location before and after the experiment.



(a) 3D view of the reconstructed image of asphaltene deposition in a microchannel (b) Deposit thickness measurement represented by color difference (μm)

Fig. 3. 3D measurement of asphaltene deposition in a microchannel (channel size: $250 \mu\text{m}$ height \times 2 mm width \times 50 mm length)

11
 12 Figure 4 shows 3D reconstructed image for both empty microchannel (Figure 4-a) and
 13 microchannel with asphaltene deposits (Figure 4-b). In both figures, a vertical and red
 14 rectangular plane is indicating the position where a two dimensional deposition profile will be
 15 measured. The corresponding two dimensional profiles are shown for empty microchannel and
 16 microchannel with deposits in figures 5-a and 5-b, respectively.

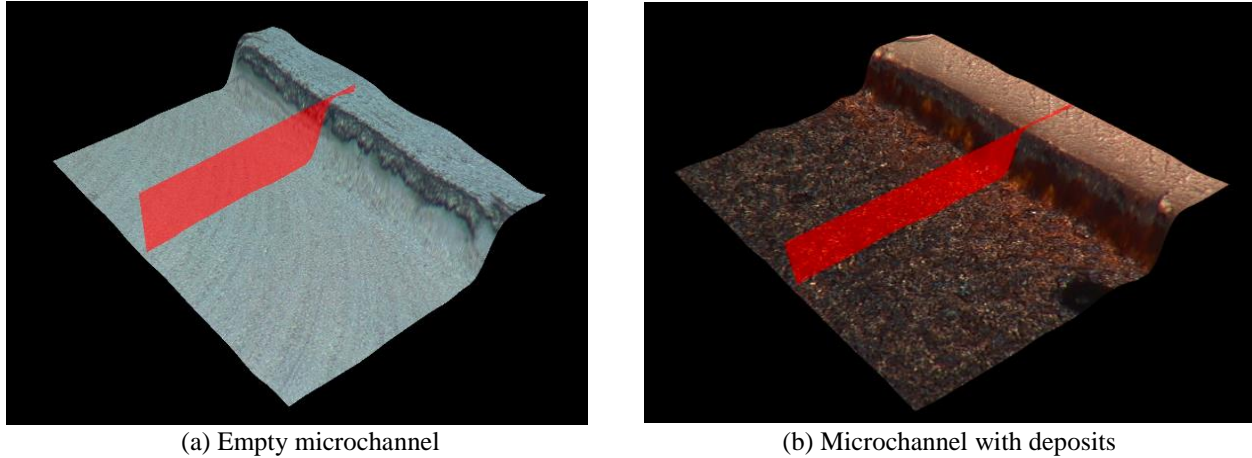
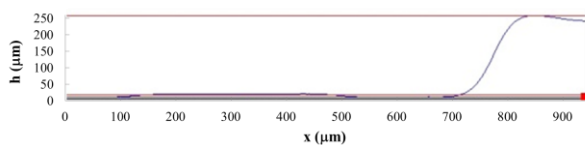
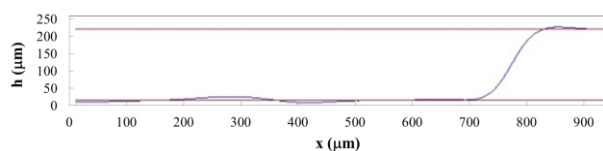


Fig. 4. 3D measurement of asphaltene deposition in a microchannel with the position indication the measurement of 2D profile (channel size: 250 μm height \times 2 mm width \times 50 mm length)

1 Figure 5-a shows that the depth of empty microchannel (D) is approximately 250 μm with
 2 an approximate roughness $\pm 12 \mu\text{m}$. The roughness of channel, due to the manufacturing process
 3 is estimated from 10 measurements taken at different positions in one microchannel and for 10
 4 empty channels at the fixed position (at the middle of channels). Figure 5-b represents the micro-
 5 channel with asphaltene deposits. The distance between deposition top and channel top is around
 6 217 μm , which means the deposition thickness (δ) is appropriately 33 μm .



(c) Empty microchannel with a maximum height of 250 μm .



(d) Microchannel with deposits with a maximum height of 217 μm .

Fig. 5. 2D profile of empty microchannel and microchannel with deposits

7 **4.2 Effect of injected volume on asphaltene deposit**

8 3D microscopy measurement is employed to study the influence of volume injection on
 9 deposit thickness by using two different experimental conditions, (i) varying the elapsed time of
 10 injection for a constant flow rate of 0.005 ml/min and (ii) changing the flow rates for a constant
 11 elapsed time of 10 hours. Both experimental results are illustrated in Figure 6. For both cases the
 12 deposit thickness of asphaltene (δ) increases with the total injection volume (V). It can be

1 observed that the amount of asphaltene deposited on the microchannel walls is too low to be
 2 measured for the total volume injection less than 4 ml and the microchannel is saturated (or
 3 blocked by the asphaltene particles) for total injection volume higher than 16 ml. The thickness
 4 range of the deposit is between 10 to 60 μm . These experimental results show that both
 5 experimental conditions obtain identical results in terms of the influence of the total injection
 6 volume.

7 Varying the elapsed time of injection for a constant flow rate of 0.005 ml/min shows that at
 8 a constant flow rate, the thickness of asphaltene deposit (δ) is growing in the microchannel. In
 9 this experiment the average velocity is $\bar{u} = 5.5 \times 10^{-4} \text{m/s}$. As it was expressed by Seifried *et*
 10 *al.* (2013) that the effect of flow rates on asphaltene deposition depended on the shear rate and
 11 therefore the magnitude of the average velocity. The range of velocity in this experiment is 10
 12 times smaller than the velocity measured by Seifried *et al.* (2013) ($\bar{u} = 6.4 \times 10^{-3} \text{m/s}$);
 13 however comparable experimental result in terms of the influence of volume injection on
 14 asphaltene deposit is obtained.

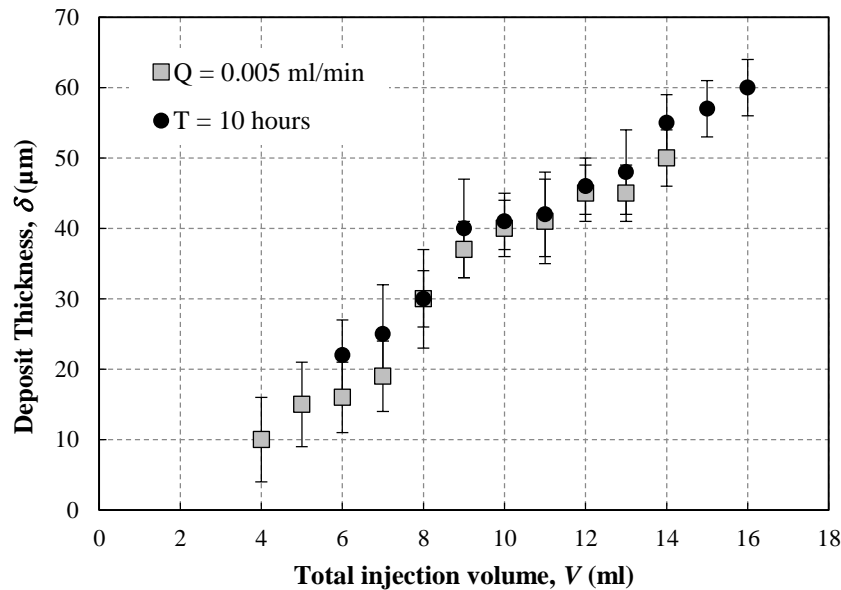


Fig. 6. Thickness measurement of Deposit thickness (δ) in terms of total injection volume V

1 Changing the flow rates for a constant elapsed time of 10 hours shows that the total
2 injection volume is increased by increasing the flow rate of the fluid mixture. Therefore, even
3 though the flow rate increases, asphaltene deposition is still increased linearly with the increasing
4 total injection volume. The average velocities in this condition are ranging from 3.3×10^{-4} to
5 $8.9 \times 10^{-4} \text{ m/s}$, which are 10 times smaller than average velocity measured by Seifried *et al.*
6 (2013).

7 The normalized deposit thickness $\delta' = \frac{\delta}{D}$ is presented versus Microchannel Volume Injection ($MVI = \frac{V}{V_c}$)
8 in Figure 7, where $D = 250 \mu\text{m}$ and $V_c = 250 \mu\text{l}$ represent the depth and the total volume of the
9 microchannel, respectively.

10

11 As showed by Figure 7, the number of MVI is ranging from 160 to 640 and the normalized
12 deposit thickness δ' increases with MVI. With the increase of the capillary volume injection, the
13 deposit thickness grows. Similar results are obtained by Lawal *et al.* (2012) even if the definition
14 of normalized deposit thickness and experimental conditions are different. Measured
15 experimental results show an approximate uniform deposition in the middle of the micro-
16 channel. However it can be observed from figure 2-a that the deposits along the micro-channel
17 might not be uniform. Further research is needed to investigate the characteristics of asphaltene
18 deposition in different locations along the micro-channel.

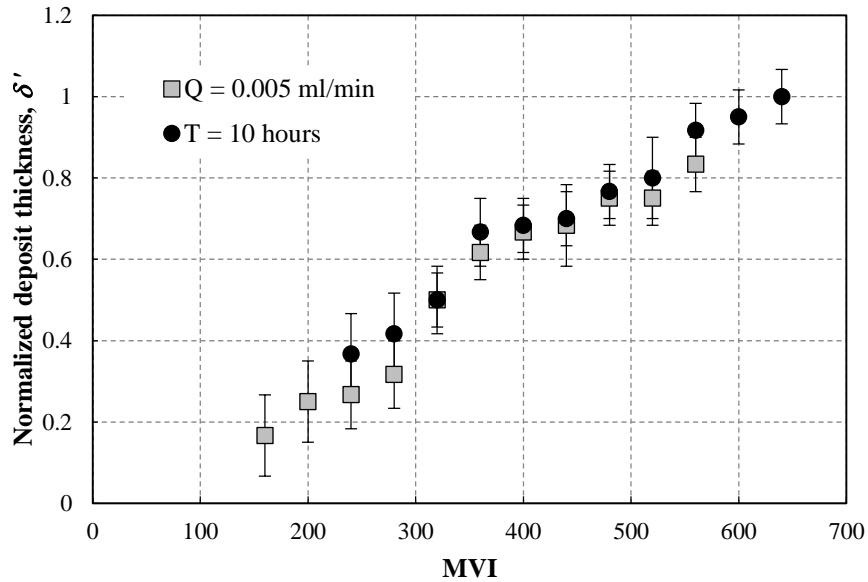


Fig. 7. Normalized deposit thickness (δ') as a function of Microchannel Volume Injection (MVI)

1

2

3 5. CONCLUSIONS

4 In this paper, experimental investigations of asphaltene deposition were carried out using

5 transparent micro-channels in the laboratory condition. A new thickness measurement method

6 for asphaltene deposits was presented using a 3D microscopy system. This method is based on

7 reconstructed images to visualize the topology of the 3D asphaltene deposition layers. The

8 thickness of the deposition layer is estimated and two-dimensional profile of the deposits is

9 measured. This new approach permits direct measurements of asphaltene deposition layer. The

10 influence of the volume injection was studied. Two experimental conditions were applied,

11 consisting of varying elapsed time or changing flow rate. Results show that continuous

12 asphaltene deposition can be represented by the change of deposition thickness, which can be

13 directly measured by the 3D digital microscope. Obtained experimental results are validated

14 using previous work of Lawal *et al.* (2012) and Seifried *et al.* (2013). The thickness of

1 asphaltene deposits increases with the increase of the total injection volume. The measured
2 thickness values range from 10 to 60 μm when the total injection volume is changed from 4 to 16
3 ml.

4 The thickness measurement method provides a new idea to measure micron-size asphaltene
5 deposition layers. The 3D microscopy technique will be used further to develop an empirical
6 model of asphaltene deposition in microchannels.

8 **AUTHOR INFORMATION**

9 *Phone: +971-26075 396. E-mail: agoharzadeh@pi.ac.ae

10 **ACKNOWLEDGMENTS**

11 The work is supported by a research grant from Abu Dhabi National Oil Company (ADNOC) through the Oil
12 Sub-Committee.

13 **REFERENCES**

- 14 Adebisi, F.M., Thoss, V., 2014. Organic and elemental elucidation of asphaltene fraction of
15 Nigerian crude oils. *Fuel* 118, 426–431.
- 16 Broseta, D., Robin, M., Savvidis, T., Féjean, C., Durandau, M., Zhou, H., 2000. Detection of
17 asphaltene deposition by capillary flow measurements, in: SPE/DOE Improved Oil
18 Recovery Symposium. Society of Petroleum Engineers. SPE-59294-MS.
- 19 Boek, E.S., Ladva, H.K., Crawshaw, J.P., Padding, J.T., 2008. Deposition of Colloidal
20 Asphaltene in Capillary Flow: Experiments and Mesoscopic Simulation†. *Energ. Fuel.*, 22
21 (2), 805–813.
- 22 Boek, E.S., Wilson, A.D., Padding, J.T., Headen, T.F., Crawshaw, J.P., 2009. Multi-scale
23 Simulation and Experimental Studies of Asphaltene Aggregation and Deposition in
24 Capillary Flow†. *Energ. Fuel.*, 24, 2361–2368.
- 25 Buckley, J.S., 2012. Asphaltene deposition. *Energ. Fuel.*, 26, 4086–4090.

- 1 Hammami, A., Phelps, C.H., Monger-McClure, T., Little, T.M., 2000. Asphaltene precipitation
2 from live oils: An experimental investigation of onset conditions and reversibility. *Energ.*
3 *Fuel.*, 14 (1), 14–18.
- 4 Hoepfner, M.P., Limsakoune, V., Chuenmeechao, V., Maqbool, T., Fogler, H.S., 2013. A
5 Fundamental Study of Asphaltene Deposition. *Energ. Fuel.*, 27 (2), 725–735.
- 6 Hu, C., Morris, J.E., Hartman, R.L., 2014. Microfluidic investigation of the deposition of
7 asphaltenes in porous media. *Lab Chip* 14 (12).
- 8 Jamialahmadi, M., Soltani, B., Müller-Steinhagen, H., Rashtchian, D., 2009. Measurement and
9 prediction of the rate of deposition of flocculated asphaltene particles from oil. *Int. J. Heat*
10 *Mass Transf.* 52 (19), 4624–4634.
- 11 Kim, S.T., Boudh-Hir, M.E., Mansoori, G.A., 1990. The Role of Asphaltene in Wettability
12 Reversal, in: SPE Annual Technical Conference and Exhibition. Society of Petroleum
13 Engineers. SPE-20700-MS.
- 14 Lawal, K.A., Crawshaw, J.P., Boek, E.S., Vesovic, V., 2012. Experimental Investigation of
15 Asphaltene Deposition in Capillary Flow. *Energ. Fuel.*, 26 (4), 2145–2153.
- 16 Mullins, O.C., 2010. The Modified Yen Model†. *Energ. Fuel.*, 24 (4), 2179–2207.
- 17 Nabzar, L., Aguiléra, M.E., 2008. The colloidal approach. A promising route for asphaltene
18 deposition modelling. *Oil Gas Sci. Technol. l’IFP* 63, 21–35.
- 19 Papadimitriou, N.I., Romanos, G.E., Charalambopoulou, G.C., Kainourgiakis, M.E., Katsaros,
20 F.K., Stubos, A.K., 2007. Experimental investigation of asphaltene deposition mechanism
21 during oil flow in core samples. *J. Pet. Sci. Eng.* 57, 281–293.
- 22 Schneider, M.H., Sieben, V.J., Kharrat, A.M., Mostowfi, F., 2013. Measurement of Asphaltenes
23 Using Optical Spectroscopy on a Microfluidic Platform. *Anal. Chem.* 85 (10), 5153–5160.
- 24 Seifried, C.M., Al Lawati, S., Crawshaw, J.P., Boek, E.S., 2013. Asphaltene Deposition in
25 Capillary Flow, in: SPE Annual Technical Conference and Exhibition. Society of Petroleum
26 Engineers, SPE 166289
- 27 Sheu, E. Y., Hammami, A., & Marshall, A. G. (Eds.), 2007. Asphaltenes, heavy oils, and
28 petroleomics, vol. 1. New York: Springer.
- 29 Shedid, S.A., Abbas, E.A.A., 2006. Reversibility of asphaltene deposition under dynamic flow
30 conditions. *Pet. Sci. Technol.* 24 (12), 1457–1467.
- 31 Wang, J., Buckley, J.S., Creek, J.L., 2004. Asphaltene deposition on metallic surfaces. *J.*
32 *Dispers. Sci. Technol.* 25 (3), 287–298.
- 33 Zendehboudi, S., Shafiei, A., Bahadori, A., James, L.A., Elkamel, A., Lohi, A., 2014. Asphaltene
34 precipitation and deposition in oil reservoirs—Technical aspects, experimental and hybrid
35 neural network predictive tools. *Chem. Eng. Res. Des.* 92 (5), 857–875.

36

1 Zhuang, Y.G., Goharzadeh, A., Yap, Y.F., Chai, J.C., Mathew, N., Lin, Y.J.N., Vargas, F.,
2 Biswal, S.L., 2015. Experimental investigation of asphaltene deposition in a transparent
3 microchannel. TFESC, New York City, USA, August.

4 Zhuang, Y.G., 2015. Asphaltene deposition in transparent mini- and micro-channels. M.Sc.
5 Thesis, The Petroleum Institute, Abu Dhabi, UAE.

6